Barriers to Internal Rotation in 1,3,5-Trineopentylbenzenes

10†—^{13}C and ^{19}F NMR Band Shape Studies and Force Field Calculations

Sven Andersson* and Torbjörn Drakenberg‡
Organic Chemistry 2, Chemical Center, University of Lund, S-220 07 Lund 7, Sweden

1,3,5-Trineopentylbenzenes (TNB) with one or two benzylic substituents in each neopentyl group were synthesized. The substituents were F, Cl, Br, I, OCH_3, $OCOCH_3$, $OSi(CH_3)_3$ and CH_3 and, in cases of disubstitution, F, Cl, Br, CH_3 and Cl, CH_3 and Br and $—SCH_2CH_2S—$. Barriers to internal C_{sp^3}–C_{sp^2} (aryl) and C_{sp^3}–C_{sp^3} rotation were estimated by ^{13}C and ^{19}F NMR band shape methods. Estimated barriers in the TNB series were found to be very close to those found for the corresponding mononeopentylbenzenes. For some of the compounds studied, molecular mechanics (MM) calculations were performed with the Allinger MMP1 program. Differences between calculated and experimental estimated barriers were found, and possible sources of these discrepancies in terms of parameters used in the MMP1 program are discussed.

INTRODUCTION

Internal rotation in the 1,3,5-trineopentylbenzene (TNB) system has been extensively studied by dynamic NMR spectroscopy.[1a–i] Most of the TNB systems hitherto studied have been substituted in the aromatic ring with halogen, alkyl, 1-hydroxyalkyl and acyl groups. On the other hand, TNB systems with benzylic substituents have rarely been studied, except for two papers by Baas and Sinnema[2] and by Martinson.[3] Martinson[3] used ^1H NMR spectroscopy to examine the spectrum of the TNB compound **14** (see below)

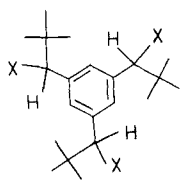

1 X= F
2 Cl
3 Br
4 I
5 OCH_3
6 $OCOCH_3$
7 $OSi(CH_3)_3$
8 CH_3

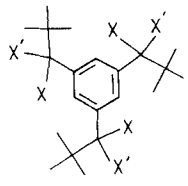

9 X = X′= F
10 X = X′= Cl
11 X = Cl, X′= CH_3
12 X = X′= Br
13 X = Br, X′= CH_3

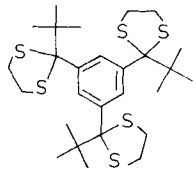

14

* Author to whom correspondence should be addressed.
† For Part IX, see Ref. 1i.
‡ Physical Chemistry 2.

between −60 °C and 60 °C, and those of TNB compounds substituted with hydrogens and hydroxyl groups and with hydroxyl and methyl groups in the benzylic positions [1,3,5-tris(1-hydroxy-2,2-dimethylpropyl)benzene and 1,3,5-tris(1-hydroxy-1,2,2,-trimethylpropyl)benzene, respectively] at 40 °C. The spectrum of the latter compound was also examined at high temperature (*ca* 200 °C). For the two hydroxyl-substituted TNB compounds, Baas and Sinnema[2] made a complementary ^1H NMR study, and discussed the low-temperature spectrum of 1,3,5-tris(1-hydroxy-1,2,2,-trimethylpropyl)benzene.

In order to extend our studies on substituent effects on the internal rotation in the TNB system, we synthesized the compounds shown above, all of which were studied as diastereomeric mixtures except, of course, the achiral compounds **9**, **10**, **12** and **14**.

EXPERIMENTAL

NMR measurements

Band shape methods were used to study barriers to internal C_{sp^3}–$C_{sp^2(aryl)}$ and C_{sp^3}–C_{sp^3} rotation. In most cases, the NMR spectra were recorded for at least ten different temperatures. The rate constants were estimated from visual fitting of plotted to experimental spectra.

In all possible cases, the transverse relaxation time (T_2) was determined at both the high and low temperature limits for the exchanging signal and a reference signal (T_2^{ref}) originating from a nucleus in the same molecule. At intermediate temperatures, T_2 was interpolated by use of Eqn (1).[4a,b]

$$T_2^{-1} = (T_2^{ref})^{-1} + \pi\Delta\nu_{corr} \qquad (1)$$

$\Delta\nu_{corr}$ is a correction factor and is assumed to vary linearly with temperature. In cases where only high

CCC-0030–4921/83/0021–0602$07.00

(low) temperature data on T_2 and T_2^{ref} could be obtained, these values were extrapolated to low (high) temperatures.

Determination of the chemical shift at temperatures where this parameter could not be estimated by band fitting was done by extrapolation from data below the coalescence temperature.

The ^{13}C NMR spectra used for band shape analysis were recorded on a Varian XL-100 spectrometer operating at 25 MHz in the Fourier transform mode. Approximately 4000 free induction decays were used to obtain a ^{13}C spectrum. The ^{19}F NMR spectra were recorded on the Varian XL-100 spectrometer operating at 94.1 MHz. The temperature was measured by means of a copper–constantan thermocouple, which was fixed near the receiver coil. The accuracy in these values has been shown to be better than ±2 °C and is reproducible within ±0.5 °C.[1b,e]

Band shape analyses involving calculations of theoretical spectra for exchange between two sites were performed on an HP 9820A calculator equipped with a plotter. The calculations of spectra for exchange among three sites were performed at the Lund University Computing Centre on a Univac 1100/80, equipped with a Calcomp plotter.

The first-order rate constants (k) obtained from the band shape analyses were used, in conjunction with the Eyring equation,[5] to calculate the free energy of activation ($\Delta G_T^{\neq}$) at each temperature (T). The rate constants were defined as $k = \tau_A^{-1}$, where τ_A is the lifetime at site A. The relative statistical errors in estimated $\Delta G_T^{\neq}$ values were estimated by the approximate expression (2), which can be derived by analysis of the Eyring equation.[6]

$$(\sigma_{\Delta G_T^{\neq}}/\Delta G_T^{\neq}) = [\ln 10(10.32 + \log T k^{-1})]^{-2}(\sigma_k/k)^2 + (\sigma_T/T)^2 \quad (2)$$

where $\sigma_{\Delta G_T^{\neq}}$, σ_k and σ_T are the relative errors in $\Delta G_T^{\neq}$, rate constant and temperature, respectively.

Calculations

Allingers MMP1[7a-g,8] molecular mechanics program was used to calculate the energy for different conformations on the potential surfaces for internal C_{sp^3}–$C_{sp^2(aryl)}$ and C_{sp^3}–C_{sp^3} rotation in compounds **9–13**.

RESULTS

The ^{13}C NMR spectra of compounds **1–14** at ambient temperature (28 °C) all showed evidence for rapidly rotating neopentyl and *tert*-butyl groups. The ^{13}C chemical shifts are summarized in Table 1.

Rotation around the C_{sp^3}–$C_{sp^2(aryl)}$ bond

For compounds **1–8**, **11** and **13**, with three chiral benzylic centres, two diastereomeric pairs are possible, the *RRR–SSS* pair and the *RRS–SSR* pair, using the Cahn–Ingold–Prelog *R,S*-nomenclature system.[9] In the case of the *RRR* or *SSS* isomer, both the unsubstituted and the substituted aromatic carbons will appear as singlets if the neopentyl groups are rotating rapidly on the NMR time scale. For the *RRS* or *SSR* isomer, these carbons may appear as doublets in a 1 : 2 (or 2 : 1) ratio. Thus, six possible signals may arise from the aromatic carbons in the ^{13}C NMR spectra of compounds **1–8**, **11** and **13**. Unfortunately, owing to very small shift differences, fewer resolvable signals have been found in all cases. At temperatures where the neopentyl rotation is slow, the aromatic region in the spectra of these chiral compounds will be very complicated, and this pattern is analyzed in detail in the discussion.

The aromatic region in the spectrum of **1** remained essentially the same down to the lowest temperature attainable (−120 °C). At temperatures where neopentyl rotation is sufficiently slow, the unsubstituted

Table 1. ^{13}C chemical shifts in benzylic substituted 1,3,5-trineopentylbenzenes (in ppm) relative to TMS (at 25 °C)

Compound	Substituted aromatic	Unsubstituted aromatic	Benzylic	Quaternary tert-butyl	tert-Butyl	Other carbons	Solvent
1	128.1	126.7	102.3	34.4	23.8	—	$CHCl_2F$
2	133.7	124.6	71.1	35.3[a]	25.2	—	CS_2–acetone-d_6(5:1)
3	135.3	125.2	65.9	35.1[a]	25.8	—	CS_2–acetone-d_6(5:1)
4	136.4	125.4	49.0	34.9[a]	26.3		CS_2–acetone-d_6(5:1)
5	136.5	125.8 125.0	90.8	34.1	24.5	55.3 CH_3 in OCH_3[a]	$CHCl_2F$
6	134.1	123.4 122.6	79.2	32.3	22.6	167.9 C=O in CH_3CO 18.6 CH_3 in CH_3CO[a]	$CHCl_2F$
7	138.1	122.3	80.0	33.5	23.1	−3.0 CH_3 in $Si(CH_3)_3$[a]	$CHCl_2F$
8	138.3	123.0	48.1	32.2	26.7	14.7 CH_3 in methyl[a]	CS_2–acetone-d_6(5:1)
9	128.4	121.0	118.5	32.6[a]	17.7	—	$CDCl_3$
10	132.0	124.1	96.9	39.4[a]	20.0	—	$CDCl_3$
11	132.5	121.5 120.5	77.7	37.6	24.6	25.2 CH_3 in methyl[a]	CS_2–acetone-d_6(5:1)
12	132.2	126.9	83.9	40.3[a]	21.0	—	$CDCl_3$
13	136.6 136.2	129.2 125.9 124.4	79.6	39.1	26.3	27.7 CH_3 in methyl[a]	CS_2–acetone-d_6 (5:1)
14	139.5	129.8	84.8	39.1[a]	27.5	37.3 CH_2 in SCH_2CH_2S	CS_2–acetone-d_6(5:1)

[a] Peaks used as internal resolution standards in band shape analyses.

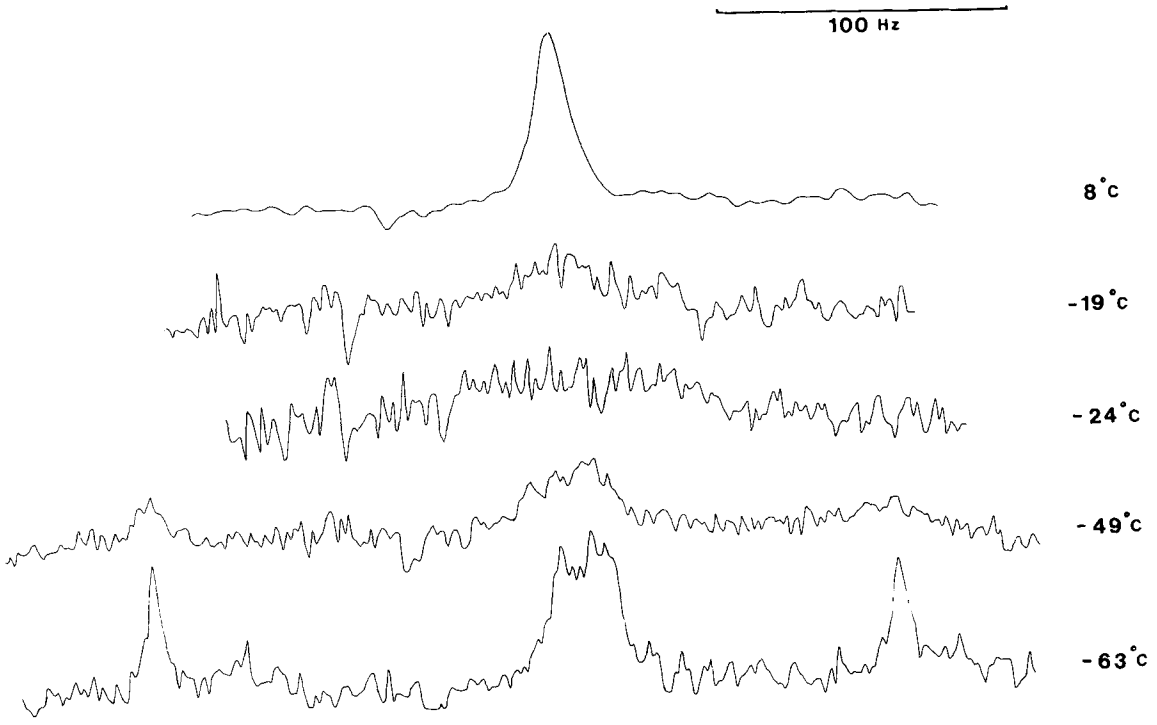

Figure 1. Temperature dependence of the unsubstituted aromatic region in the ^{13}C NMR spectrum of compound **4** in CS_2–acetone-d_6 (5:1) solution.

aromatic carbon region in the ^{13}C spectra of the halogen-substituted compounds **2–4** clearly shows substituent effects. When the benzylic substituents are iodine (**4**), very large shift differences are found, and four signals are resolvable (Fig. 1).

If bromines are the substituents (**3**), the shift differences found are less and three peaks are resolvable, and when chlorines are the substituents (**2**) the shift differences are so small that only one peak is observed. In the latter case, also at sufficiently slow neopentyl rotation, the substituted aromatic carbons showed three signals which could be used for band shape analysis.

At temperatures where the neopentyl rotation is sufficiently slow, the unsubstituted aromatic carbon regions in the spectra of the oxygen-containing compounds **5–7** all show similar three-peak patterns. The chemical shift differences observed in all cases are greater than those observed when bromines are the benzylic substituents.

When the benzylic substituents are methyl groups (i.e. **8**), very large chemical shift differences are observed for the unsubstituted aromatic carbons at slow neopentyl rotation (Fig. 2). The chemical shift differences in this case are of the same magnitude as those observed when iodines are the benzylic substituents. The shift differences observed for **8** are remarkable, since it has been observed that, for the corresponding mononeopentylbenzenes,[10] the methyl-substituted compound exhibits a chemical shift difference between the *ortho*-carbons which is only *ca* half of that observed for the iodo-substituted compound. The reason for the large differences observed for **8** is not yet clear.

Three signals from the unsubstituted aromatic carbons are observed at ambient temperature for the bromo-substituted compound **13**; Fig. 3. For the chloro-substituted compound **11**, the chemical shift differences are smaller, and only two signals are observed. At slow neopentyl rotation the two partly overlapping signals in Fig. 3 (at 125.9 and 124.4 ppm, **13**) are split into three signals of similar magnitude, as observed in the case of **11**.

The aromatic carbon region in the ^{13}C NMR spectra of the achiral compounds **9**, **10**, **12** and **14** is expected to consist of two singlets, one from the unsubstituted and one from the substituted aromatic carbons, as

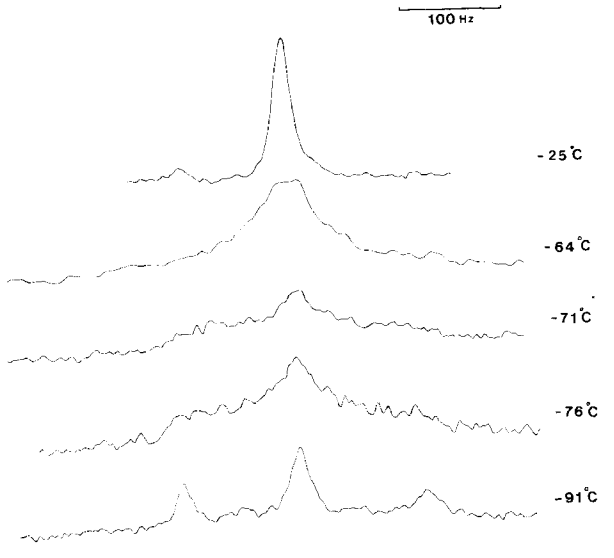

Figure 2. Temperature dependence of the unsubstituted aromatic region in the ^{13}C NMR spectrum of compound **8** in CS_2–acetone-d_6 (5:1) solution. The small peak at the left (−25 °C) is an impurity.

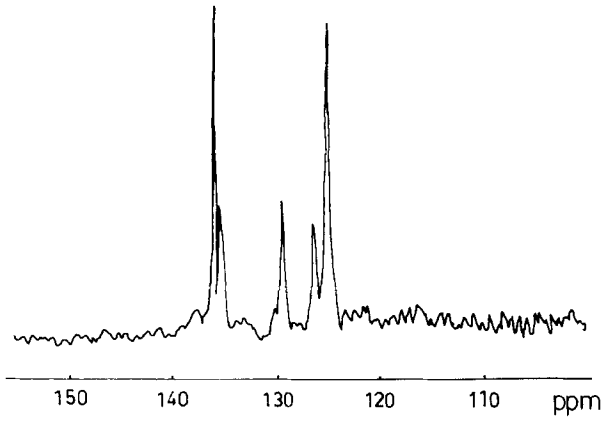

Figure 3. Aromatic region of the ^{13}C NMR spectrom of **13** in CS_2–acetone-d_6 (5:1) solution at ambient temperature.

observed (Table 1). The aromatic region in the spectra of **10**, **12** and **14** remained essentially the same down to the lowest temperatures attainable (−156 °C for **10**, −153 °C for **12** and −125 °C for **14**).

^{19}F NMR measurements

The ^{19}F NMR spectrum of **9** in $CHCl_2F$ solution is shown in Fig. 4. At high temperatures, when the neopentyl rotation is rapid, only one signal is expected from the benzylic fluorines, as found. At temperatures where the neopentyl rotation is sufficiently slow, however, two rotamers will exist. In one rotamer, all three *tert*-butyl groups are on the same side of the ring plane ('rotamer D'[1j]) and in this rotamer all fluorines will, of course, give rise to a singlet. In the other rotamer, with two *tert*-butyl groups on one side of the ring plane and one on the other (three identical rotamers, 'A = B = C'[1j]), the fluorines will give rise to two AB quartets with an intensity ratio 1 : 2. Owing to solubility problems at low temperatures, neither of the expected AB quartets could be resolved. However, the two outermost signals at −152 °C (Fig. 4) are very broad and have the approximate ratio 1 : 2.

To estimate $\Delta G_T^{\neq}$ for **2–8**, **11** and **13**, an approximate band shape method involving a three-site case

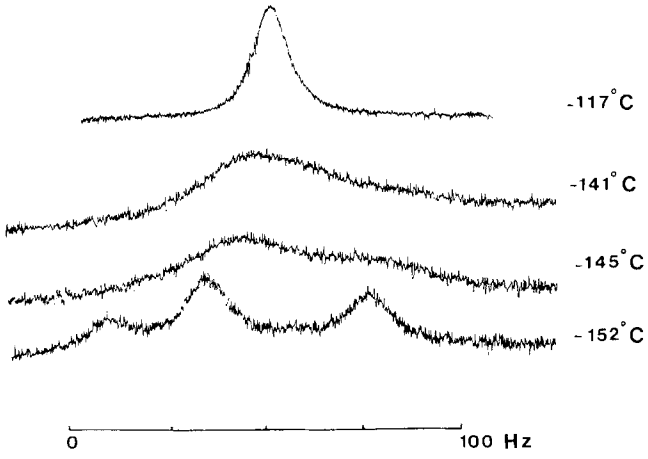

Figure 4. Temperature dependence of the ^{19}F NMR spectrum of **9** in $CHCl_2F$ solution.

Table 2. ^{13}C (and ^{19}F) chemical shift differences ($\Delta\nu$) and calculated free energies of activation ($\Delta G_T^{\neq}$) for the neopentyl rotation in some benzylic substituted TNB compounds

Compound	$\Delta\nu$(Hz)	$\Delta G_T^{\neq}$(kJ mol^{-1})[T(°C)][a]	Solvent
2	28.0 22.0 ±1.0	37.5±0.9 (−86)	CS_2–acetone-d_6 (5:1)
3	57.5 35.5 ±1.5	41.7±1.3 (−54)	CS_2–acetone-d_6 (5:1)
4	147.5 108.5 ±1.0	47.8±1.1 (−24)	CS_2–acetone-d_6 (5:1)
5	61.9 61.0 ±1.5	41.1±1.2 (−41)	CS_2–acetone-d_6 (5:1)
6	59.0 54.0 ±2.0	36.8±1.3 (−73)	CS_2–acetone-d_6 (5:1)
7	59.2 38.5 ±1.0	36.3±1.0 (−63)	CS_2–acetone-d_6 (5:1)
8	115.0 123.0 ±1.5	39.3±1.0 (−64)	CS_2–acetone-d_6 (5:1)
9	25.0 41.0 ±2.0[b]	25.8±1.2 (−141)	$CHCl_2F$
11	62.0 61.0 ±2.0	33.4±1.2 (−91)	CS_2–acetone-d_6 (5:1)
13	80.0 56.0 ±2.0	37.5±1.0 (−82)	CS_2–acetone-d_6 (5:1)

[a] Error in temperature ±2 °C.
[b] ^{19}F chemical shift differences.

was used (see Discussion). The values are summarized in Table 2. The signals used as internal resolution standards are noted in Table 1, except for **9**, where one of the solvent ($CHCl_2F$) peaks was used.

C_{sp^3}–C_{sp^3} Rotation

By analogy with the case of *tert*-butyl rotation in mononeopentylbenzenes,[10] the *tert*-butyl resonances in the chiral compounds **1–8**, **11** and **13** are expected to split into three signals of equal intensities when the *tert*-butyl rotation is sufficiently slow. However, for compounds **2–8** and **13** only 1 : 2 doublets were observed, evidently as the result of chemical shift equivalence between two of the three ^{13}C methyl resonances.

For compounds **1** and **11**, the *tert*-butyl resonances remained as singlets down to the lowest temperatures attainable (−120 °C for **1** and −105 °C for **11**).

For the achiral compounds **9**, **10**, **12** and **14**, the *tert*-butyl resonances are expected to split into two signals in the ratio 1 : 2 when *tert*-butyl rotation is slow, because two of the three methyl groups will reside in identical chemical environments. This was observed, and is exemplified in Fig. 5 for **12**.

Band shape analysis

To estimate the *tert*-butyl rotation rate for compounds **2–10** and **12–14** the spectra were simulated as two-site cases with a 1 : 2 population ratio, and the rate constant for the low population site was used to calculate $\Delta G_T^{\neq}$. For the diastereomeric compounds **2–8** and **13** this is a simplified treatment, but it can be justified since every 120° twist of the *tert*-butyl group will

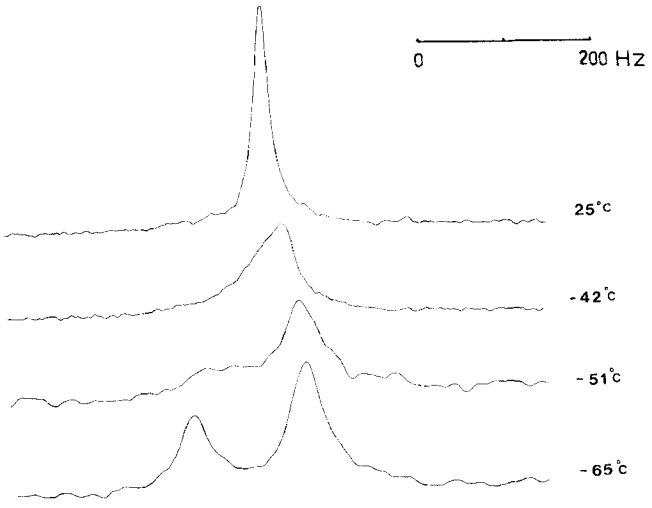

Figure 5. Temperature dependence of the methyl resonances in the *tert*-butyl groups in the ^{13}C NMR spectrum of **12** in chloroform-*d* solution.

change the environment of the low population site, whereas only every second 120° twist will change the environment of the two carbons with the same shift.

The signals used as internal resolution standards are noted in Table 1.

From the estimated rate constants (k) the free energies of activation ($\Delta G_T^{\neq}$) were calculated. The results are summarized in Table 3.

DISCUSSION

By analogy with the work of Baas and Sinnema[2] on the chiral compound 1,3,5-tris(1-hydroxy-1,2,2-trimethylpropyl)benzene, two diastereomeric pairs are possible. One pair consists of a mixture of *RRR* and *SSS* enantiomers, while the other is a mixture of *RRS* and *SSR* enantiomers. In Fig. 6, this is exemplified for **4**, but only one of the two possible enantiomers for each diastereomer (Ia and IIa) is shown.

Table 3. ^{13}C chemical shift differences ($\Delta\nu$) and calculated free energies of activation ($\Delta G_T^{\neq}$) for the *tert*-butyl rotation in some benzylic substituted TNB compounds

Compound	$\Delta\nu$(Hz)	$\Delta G_T^{\neq}$(kJ mol^{-1}) [T(°C)][a]	Solvent
2	195.0±2.5	31.8±0.5 (−99)	$CHCl_2F$
3	90.0[b]	35.2±0.8 (−94)	CS_2–acetone-d_6 (5:1)
4	130.0[b]	35.3±0.6 (−91)	CS_2–acetone-d_6 (5:1)
5	174.0±2.5	27.5±0.8 (−108)	$CHCl_2F$
6	131.0±2.0	28.4±0.8 (−109)	$CHCl_2F$
7	150.0±3.0	34.3±1.0 (−102)	$CHCl_2F$
8	130.0±2.0	27.9±0.8 (−115)	CS_2–acetone-d_6 (5:1)
9	52.0±1.0	28.2±0.7 (−132)	$CHCl_2F$
10	39.1±0.6	44.9±0.7 (−56)	$CDCl_3$
12	131.8±0.8	49.7±0.9 (−42)	$CDCl_3$
13	97.7±0.7	43.3±1.2 (−62)	CS_2–acetone-d_6 (5:1)
14	14.0±1.5	35.9±1.3 (−106)	$CHCl_2F$

[a] Uncertainty in temperature ±2 °C.
[b] Estimated shift differences from broadenings below coalescence, because low-temperature spectra could not be obtained owing to solubility problems.

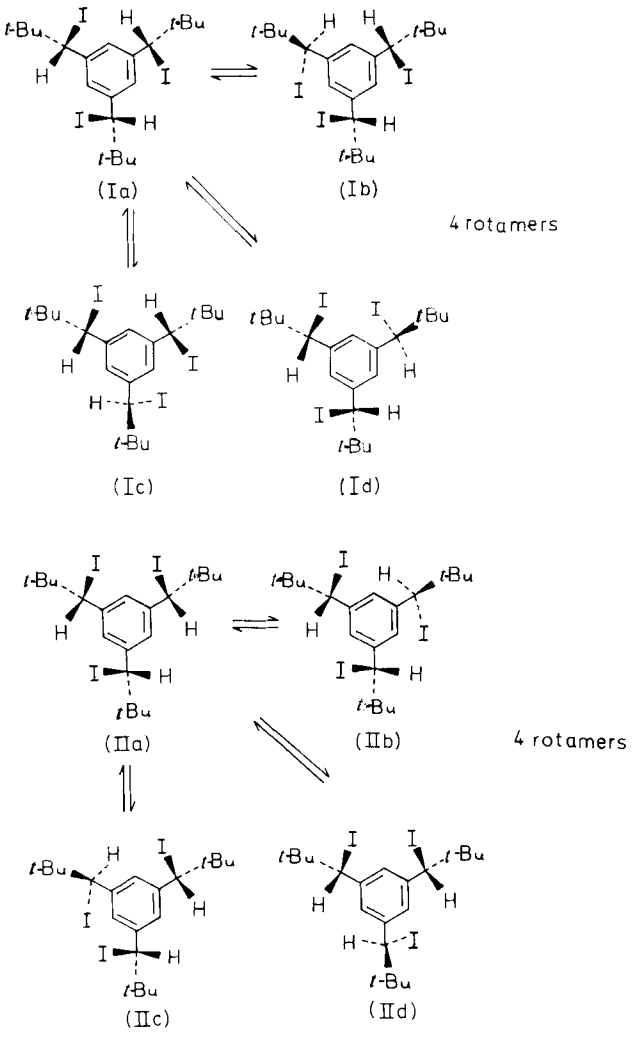

Figure 6. Different rotamers of the *SSS* and *SSR* enantiomers of **4**.

The unsubstituted aromatic carbon region in the ^{13}C NMR spectrum of **4** at temperatures where neopentyl rotation is slow will be analysed. An analysis of the substituted aromatic carbon region or the benzylic carbon region could also be performed, but in most cases the shift differences observed from these regions are smaller than those observed from the unsubstituted aromatic carbon region. The analysis is, of course, not restricted to **4**, but is general for all of the chiral compounds studied (**1**–**8**, **11** and **13**).

In rotamer Ia (Fig. 6), which is the *SSS* enantiomer, all unsubstituted aromatic carbons will have the same chemical shift ν_{IH}, since each carbon is situated between one benzylic iodine and one benzylic hydrogen. Rotation of each of the neopentyl groups in rotamer Ia by 180° gives rise to rotamers Ib, Ic and Id. In each of these rotamers, all of the unsubstituted aromatic carbons will have different chemical shifts. One of the unsubstituted aromatic carbons in rotamers Ib, Ic and Id will have the chemical shift ν_{IH} (as in rotamer Ia) but the other two, situated between two benzylic protons or two benzylic iodines, will have the chemical shifts ν_{HH} or ν_{II}, respectively, which are upfield and downfield, respectively, relative to ν_{IH}.[11] It is then assumed that the chemical shift for an aromatic carbon

will be the same (or there will be very little difference) if the two proximate benzylic iodines, protons or *tert*-butyl groups are on the same or opposite sides of the ring plane.

In rotamer IIa (the *SSR* enantiomer) the unsubstituted aromatic carbons will have three different chemical shifts situated at ν_{II}, ν_{HH} and ν_{IH}. A 180° rotation of the neopentyl group with the *R* configuration in rotamer IIa gives rise to rotamer IIb. In this rotamer, the three unsubstituted aromatic carbons will all have the same chemical shift, centred at ν_{IH}. However, if each of the two neopentyl groups with the *S* configuration in rotamer IIa is rotated by 180°, rotamers IIc and IId are formed. The chemical shifts for the unsubstituted aromatic carbons will all be different in both rotamers, by analogy with rotamer IIa. The net result is then six signals centred at ν_{II}, twelve at ν_{IH} and six at ν_{HH}. However, before we can predict the intensity ratios in the ^{13}C NMR spectrum of **4**, the statistical probability must be taken into account. If a statistical probability of 50% is assumed for the production of a chiral benzylic centre with *R* configuration, there will be a 25% total probability for the formation of the *RRR* and *SSS* enantiomers. There will then be a 75% total probability for the formation of the *RRS* and *SSR* enantiomers. If the differential effect of *tert*-butyl groups on opposite sides of the ring plane is neglected, the unsubstituted aromatic carbon region in the spectrum of **4**, at temperatures where neopentyl rotation is slow, may be roughly predicted to consist of three signals centred at ν_{II}, ν_{IH} and ν_{HH}, with the relative intensities 1 : 2 : 1.

From the discussion above, it is clear that a band shape method involving simulation as a three-site case should be a good approximation here. However, some restrictions on the general three-site case are necessary: (i) only the exchanges $\nu_{II} \rightleftarrows \nu_{IH}$ and $\nu_{IH} \rightleftarrows \nu_{HH}$ are considered, and (ii) no direct exchange is allowed between ν_{II} and ν_{HH}. Further, the populations at sites ν_{II} and ν_{HH} will be equal. In all spectra of the chiral compounds (**2–8**, **11** and **13**) the relative intensities 1 : 1.9 : 1 to 1 : 2.6 : 1 were found from band shape analysis. A divergence from 1 : 2 : 1 shows that not all of the rotamers in Fig. 6 are equally populated, i.e. some of them are preferred.

For the achiral compounds **10**, **12** and **14** at temperatures where the neopentyl rotation is slow, the aromatic ^{13}C NMR spectrum will consist of three signals from the unsubstituted and three from the substituted aromatic carbons. This will be the result of the presence of the two rotamers D and A = B = C.[1j] In the above discussion of the diastereomeric systems, it was assumed that the location of the halogens, hydrogens or *tert*-butyl groups with respect to the ring plane had little or no effect on the shifts of the unsubstituted aromatic carbons. In the case of achiral compounds, this is the *only* effect when the neopentyl rotation is slow. It is thus not surprising that no shift effects could be detected for **10**, **12** and **14**.

C_{sp^3}–C_{sp^2}(aryl) rotation

The trend in barriers estimated for the neopentyl rotation in the TNB compounds **2–8** (Table 2) is in good agreement with that previously found for similarly substituted mononeopentylbenzenes.[10] This is expected if the steric attractive effects in the TNB system[1g,i,j] are left out of consideration. Table 2 also shows that, within experimental error, the neopentyl barriers found in the TNB system are the same as those previously found in the mononeopentylbenzene[10] system.

Table 4. Barriers to internal neopentyl rotation (kJ mol^{-1}) for some benzylic- and ring-substituted TNB compounds

Compound	$\Delta G^{\neq}$ [a]	Compound	$\Delta G^{\neq}$ [a]
1	—	2,4-F_2-TNB	37.6
2	37.5	2,4-Cl_2-TNB	61.6
3	41.7	2,4-Br_2-TNB	69.5
4	47.8	2,4-I_2-TNB	78.7
8	39.3	2,4-Me_2-TNB	64.5

[a] $\Delta G^{\neq}$ values obtained at one temperature.

Nilsson *et al.*[1d–f] have estimated barriers to internal neopentyl rotation in the ring-substituted compounds 2,4-difluoro-, 2,4-dichloro-, 2,4-dibromo-, 2,4-diiodo- and 2,4-dimethyl-TNB. Their results are collected in Table 4, together with the results from measurements on the benzylic-substituted compounds **2–4** and **8**.

The barrier to internal neopentyl rotation in **1** could not be estimated from ^{13}C NMR spectra. Table 4 shows that there is good agreement between the trends in the two series, although the barriers found for the benzylic-substituted TNB compounds are lower than those for ring-substituted TNB compounds.

In a study of internal rotation in mononeopentylbenzenes,[10] it was found that the neopentyl barrier decreases when the benzylic proton in 1-phenyl-1-X-2,2-dimethylpropane (X = Cl or *tert*-Bu) was substituted for a chlorine or a *tert*-butyl group. The neopentyl barriers could only be estimated for **9**, **11** and **13**. Comparison of the $\Delta G^{\neq}$ values estimated for neopentyl rotation in **2**, **3**, **8**, **11** and **13** (Table 2) shows that if benzylic methyl groups are introduced in **2** and **3**, the neopentyl barriers decrease by about 4 kJ mol^{-1}. When benzylic chlorines are introduced in **8**, the barrier decreases by about 6 kJ mol^{-1} and when benzylic bromines are introduced a very small change is found. Anderson *et al.*[12] observed, by ^{1}H NMR, a decrease in neopentyl barriers of 5.0 and 5.8 kJ mol^{-1} when the benzylic protons in *para*-NO_2- and *para*-OCH_3-substituted 1-phenyl-1,2,2-trimethylpropane were replaced by chlorines. They explained the decrease in the barrier as due to the destabilization of the initial state when the benzylic hydrogen is replaced by a chlorine. This will then lead to a decreased barrier to internal rotation, provided the transition state is only slightly affected by the replacement. This explanation is also valid in the work of Rieker and Kessler,[13] who observed a decreased barrier to internal rotation when tertiary protons in sterically hindered fluorenyl and triarylmethyl systems were replaced by bulkier groups, such as hydroxyl and chlorine.

In an attempt to elucidate further the barriers in **9–13**, MM calculations with the Allinger MMP1 program[7a–g] were performed. For all compounds, the

Table 5. Calculated steric energies (E_{Steric}), dipole energies (E_{Dipole}) for some conformations on the potential curve for internal neopentyl rotation and total energy differences (ΔE_{Total}) in kJ mol^{-1} for benzylic-substituted TNB compounds (see text)

Compound	A[a]		B[b]		C[c]		D[d]		E[e]
	E_{Steric}	E_{Dipole}	E_{Steric}	E_{Dipole}	E_{Steric}	E_{Dipole}	E_{Steric}	E_{Dipole}	ΔE_{Total}
9	93.6	2.3	91.4	7.0	123.8	3.4	119.9	4.4	31.3
10	179.1	3.1	181.1	7.4	214.5	5.6	202.7	5.1	37.9
11	202.3	1.9	204.4	1.3	239.5	2.0	232.5	1.9	37.3
12	206.3	3.9	208.5	9.0	248.5	7.6	228.0	6.1	45.9
13	222.4	1.8	224.0	1.1	264.5	1.8	251.9	1.9	42.1

[a] A: initial state (rotamers A = B = C). For compounds **11** and **13** see text.
[b] B: rotamer D.
[c] C: transition state.
[d] D: the rotamer with one neopentyl twisted by 90° from the conformation in rotamer D.
[e] E: calculated barrier.

MM calculations were carried out on the rotamer with all three *tert*-butyl groups on the same side and perpendicular to the ring plane ('rotamer D'[1j]). For the chiral compounds **11** and **13** only the *RRR* (or *SSS*) isomer was used for calculations. One of the neopentyl groups in rotamer D was rotated by 180° to a conformation corresponding to rotamers A, B and C. Some points along the calculated potential curves are given for compounds **9–13** in Table 5, where the steric (E_{Steric}) and electrostatic (E_{Dipole}) contributions to the total energy ($E_{Total} = E_{Steric} + E_{Dipole}$[7g]) are separated.

For all compounds, rotamers A, B and C were found to be the most stable. In the case of **9** this is in accord with the results from band shape analysis, where an isomer ratio D/(A, B and C) = 2/3 was estimated. If the dipolar contribution (E_{Dipole}) to the total energy sum is subtracted, rotamer D is found (as in the case of TNB itself[1i,j]) to have the lowest energy for all compounds (Table 5).

The potential curve calculated for **9** and **10** on rotating a neopentyl group by 180° in rotamer D has, in both cases two maxima (of equal height), situated when the rotating group is twisted 24° out of the ring plane on either side. The other two neopentyls are still on the same side and perpendicular to the ring plane. For **11**, **12** and **13** the potential curves also have two peaks, but of unequal heights. The maximum is in all cases found when the rotating neopentyl is on the same side of the ring plane as the other two, and is twisted 33°, 35° and 38°, respectively, out of the ring plane. The calculations for compounds **9–13** show (Table 5) that if the dipolar contribution (E_{Dipole}) is subtracted from the total energy (E_{Total}) at each point along the potential curve, a potential curve similar to that reported for TNB[1i] will be found in all cases.

In the case of **10** the potential curve was also calculated when one of the neopentyls on the same side of the ring plane in rotamers A, B and C was rotated by 180°. A potential curve with two peaks of nearly the same height (difference only 2 kJ mol^{-1}), situated when the rotating group is 30° above or below the ring plane, was found. The barrier to internal neopentyl rotation, calculated as the energy difference between the highest and the lowest point on the potential curve, is 38 kJ mol^{-1}. This is equal to the barrier calculated when one of the neopentyls in rotamer D was rotated by 180° (cf. Table 5). If the dipolar contribution (E_{Dipole}) is subtracted from the total energy (E_{Total}) at each point along the potential curve, a new curve will be found which is similar to that reported for the same rotation in TNB.[1i]

The energy differences (ΔE_{Total}) calculated in Table 5 may thus be regarded as the barriers to internal neopentyl rotation in **9–13**. Tables 2 and 5 show that barriers calculated for **9**, **11** and **13** are about 4–6 kJ mol^{-1} higher in energy than those measured. The calculations also show that when the benzylic methyl groups in **13** are replaced by the larger bromines (**12**), the barrier increases by 3.8 kJ mol^{-1} (see Table 5). The theoretical results in a previous study on mononeopentylbenzenes[10] indicate that the barrier to internal C_{sp^3}–$C_{sp^2(aryl)}$ rotation decreases when the effective size of the third substituent increases, and this result is experimentally verified above (cf. neopentyl barriers for **8**, **11** and **13**). From the literature[7g,14–16] it is known that one of the most crucial problems with the MM1/MMP1 program is to obtain reliable results on halogen-substituted compounds. For monohalogenated alkanes, the MM1/MMP1 program gives acceptable results, but for compounds with two or more halogens, and especially in the case of geminal halogens, the program does not give reliable results.[14,15]

In addition, the MM1/MMP1 program does not contain constants for benzylic halogens in the expressions for the calculation of the torsional energy ($E_{Torsion}$) and bending energy (E_{Bend}) contributions to the total energy (E_{Total}).[7g,14] The torsional constant (V_3) and the bending constants (θ_0 and k_b) used have therefore been approximated to those estimated for halogenated alkanes. The constants used are given in Table 6.

Another problem concerns the contribution of the electrostatic term (E_{Dipole}) to the total energy. The electrostatic term in the MM1/MMP1 program has the form[14]

$$E_{Dipole}(\text{kJ mol}^{-1}) = 14.39418 \times 4.187\mu_A\mu_B(\cos\chi - 3\cos\alpha_A\cos\alpha_B)/r^3d$$

where μ_A and μ_B are bond moments, d is the dielectric constant and $\vec{r}$ is taken as connecting the midpoint

Table 6. Torsional and bending constants used in the MM1/MMP1 program

Constants	Angle	V_1(kJ mol^{-1})	V_2(kJ mol^{-1})	V_3(kJ mol^{-1})
Torsional[a]	C_{sp^2}–C_{sp^2}–C_{sp^3}–F	0.0	68.04	2.97
	C_{sp^2}–C_{sp^2}–C_{sp^3}–Cl	0.0	68.04	3.35
	C_{sp^2}–C_{sp^2}–C_{sp^3}–Br	0.0	68.04	3.35

Constants	Angle	θ_0(°)	k_b(mdyn Å rad^{-2})
Bending[b]	C_{sp^2}–C_{sp^3}–F	109.2	1.22
	C_{sp^2}–C_{sp^3}–Cl	109.8	0.96
	C_{sp^2}–C_{sp^3}–Br	109.1	0.90

[a] $E_{Torsion}(\text{kJ mol}^{-1}) = \frac{V_1}{2}[1+\cos(w)] + \frac{V_2}{2}[1-\cos(2w)] + \frac{V_3}{2} \times [1+\cos(3w)]$.
[b] $E_{Bend}(\text{kJ mol}^{-1}) = 0.021914 \times 4.187\ k_b(\theta-\theta_0)^2[1+C_f(\theta-\theta_0)]$, $C_f = -0.006$.

of the bond that defines $\vec{\mu}_A$ with that of $\vec{\mu}_B$. The angles χ, α_A and α_B are between $\vec{\mu}_A$ and $\vec{\mu}_B$, $\vec{\mu}_A$ and $\vec{r}$, $\vec{\mu}_B$ and $\vec{r}$, respectively. The bond moment factors (μ) and the dielectric constant (d) used in the program have been derived from measurements on halogenated alkanes (containing between two and six carbons) and on halogenated cyclohexanes, since experimental results are available only for these simple systems[7g,14,15]. In view of these limitations, the calculations of energy differences for **9–13** must be regarded as very approximate.

C_{sp^3}–C_{sp^3} rotation

The barriers for the internal *tert*-butyl rotation in **2–8** (Table 3) are, as expected, equal within experimental error to those previously found for the corresponding mononeopentylbenzenes.[10] Table 3 also shows that the barrier to internal *tert*-butyl rotation increases as the third benzylic substituent increases in size. The *tert*-butyl barriers found for **10**, **12** and **13** are in very good agreement with the results of Hawkins *et al.*[17] and those of Anderson and Pearson[18a–e] on the internal rotation in 1,1-dihalo- and 1-halo-1-methyl-substituted ethanes. The *tert*-butyl barriers observed (Table 3) are of purely steric origin, and the initial and transition states are probably staggered and eclipsed conformations. These conformations were also proposed by Hawkins *et al.*[17]

The barriers to internal *tert*-butyl rotation in **9–13** were calculated with the MMP1 program. In the calculations, the TNB molecule had the structure of rotamer D. For the chiral compounds **11** and **13**, calculations were only performed on the *RRR* (or *SSS*) isomers. The results are collected in Table 7, where the total steric energy (E_{Total}; see above) for the molecule is presented, together with different values of

Table 7. Total energy (E_{Total}), the angle (γ) between a benzylic halogen and a methyl group in the rotating *tert*-butyl group and calculated *tert*-butyl barriers (ΔE_{Total}) for some benzylic-substituted TNB compounds

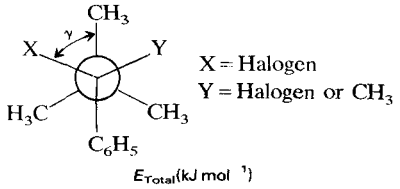

X = Halogen
Y = Halogen or CH_3

	E_{Total}(kJ mol^{-1})				
γ(°)	9	10	11	12	13
68	—	—	204.5	—	224.4
62	98.4	188.5	205.4	217.6	225.1
52	99.2	189.6	208.2	219.2	228.2
42	101.1	192.9	210.6	222.0	230.5
32	104.8	196.7	221.5	226.2	240.3
22	108.6	202.0	214.4	232.0	236.1
12	113.5	210.1	220.5	240.6	242.1
4	116.9	216.0	227.2	246.2	248.6
1	117.7	217.4	—	248.1	—
ΔE_{Total}	19.3	28.9	22.7	30.5	24.2

Table 8. Different energy contributions (ΔE_x in kJ mol^{-1}, see text) to the calculated C_{sp^3}–$C_{sp^2(aryl)}$ and C_{sp^3}–C_{sp^3} barrier in 11

Energy contribution	C_{sp^3}–$C_{sp^2(aryl)}$	C_{sp^3}–C_{sp^3}
$\Delta E_{Compression}$	5.8	2.6
$\Delta E_{Bending}$	8.2	7.2
$\Delta E_{Stretch-bend}$	0.5	0.3
$\Delta E_{Van\ der\ Waals\ (vdW)}$	14.9	10.5
$\Delta E_{Torsion}$	8.7	3.0
$\Delta E_{Torsion-bend}$	−0.7	−0.9
ΔE_{Dipole}	−0.1	−0.1

the dihedral angle (γ) between a benzylic halogen and a methyl group in the rotating *tert*-butyl.

As expected, the calculations show that staggered and eclipsed conformations are the initial and transition states, respectively. There is a striking similarity between the trends in calculated and measured *tert*-butyl barriers, although those calculated are much smaller. Similar discrepancies have been reported by Freitag and Schneider,[16] who calculated *tert*-butyl barriers (with the MM1 program) in monosubstituted neopentanes which are 3–6 kJ mol^{-1} less than those observed from experiments. On the other hand, the MMP1 program has been reported to calculate methyl barriers (in triptycenes) that are greater than those observed experimentally,[19] and calculated C_{sp^3}–$C_{sp^2(aryl)}$ barriers in mononeopentylbenzenes[10] and TNB compounds[11] (see above) are also greater than those observed experimentally. For **11** the calculations of the neopentyl and the *tert*-butyl barrier were more carefully inspected. The different energy contributions [$\Delta E_x = E_x$(transition state) − E_x (initial state)] to the calculated barriers are summarized in Table 8.

The calculations show that for *tert*-butyl rotation, the barrier is dominated by van der Waals energy, due to interactions between the hydrogens of the *tert*-butyl group and the surroundings, and by the bending energy. For the C_{sp^3}–$C_{sp^2(aryl)}$ barrier, van der Waals and bending energies are still two large contributions. In addition to these energy sums, a relatively large torsional energy contribution (8.7 kJ mol^{-1}) is found, due to torsion along the benzylic bond connecting the rotating neopentyl with the aromatic ring. In the case of *tert*-butyl rotation, on the other hand, the torsional energy amounts to less than half of the bending energy. The compression energy, due to stretching forces in the twisting bonds, is also of greater importance in the case of neopentyl rotation than for *tert*-butyl rotation.

It is difficult to predict which parameter(s) (in the MM1/MMP1 program) should be changed to obtain theoretical results in better accord with the experimental results obtained here. A parameter which may be very important for the results is the interacting radius ($r_{C\cdots H}$) for the hydrogen nucleus which is equal to 0.925 × C—H bond distance in the MM1/MMP1 program. The Allinger MM2[15,20]/MMP2 program, which uses smaller and softer hydrogens ($r_{C\cdots H} = 0.915 \times$ C—H bond distance), has been shown to give geometries for sterically hindered systems, such as the di- and tri-*tert*-butylmethane systems, which are in better accord with crystallographic data than those from the

MM1/MMP1 program.[15] However, Beckhaus *et al.*[21] have calculated barriers in hindered ethanes, with the MM1 and MM2 programs, that are very similar. Both programs also give barriers that are smaller than those observed in NMR experiments.

The size of the methyl group

The order of the estimated C_{sp^3}–$C_{sp^2(aryl)}$ barriers in the TNB compounds **2**, **3** and **8** (i.e. Cl, Br and CH_3 as substituents) is **2**<**8**<**3** (Table 2). This indicates that the relative sizes of the substituents in this system follow the order Cl<CH_3<Br, which is in agreement with measurements by Nilsson *et al.*[1f] on ring-substituted TNB compounds. However, estimated C_{sp^3}–C_{sp^3} barriers show the order CH_3<Cl<Br (Table 3), which is in agreement with measurements on substituted ethanes.[16,22] This illustrates the points made by Nilsson *et al.*[1f] and by Mislow *et al.*,[22] namely that the trends depend on the molecular system involved and the methyl, chloro and bromo groups are not strictly comparable. The chloro and bromo groups have local $C_{\infty v}$ (conical) symmetry, i.e. they are 'pear-shaped', whereas the methyl group has local C_{3v} symmetry, i.e. it is 'three pronged'.[22]

CONCLUSIONS

This work shows that barriers to internal rotation in benzylic substituted TNB compounds are similar to those found for the corresponding mononeopentylbenzenes.[10] It was also found that the attractive steric effects suggested as operating in the TNB system[1g,i,j] are completely dominated by electrostatic effects when the TNB molecule contains benzylic halogens. In these cases rotamer 'A=B=C'[1i,j] was found to be the most stable.

From estimated C_{sp^3}–$C_{sp(aryl)}$ and C_{sp^3}–C_{sp^3} barriers in compounds with benzylic Cl, Br and CH_3 groups, two different orders of relative sizes (Cl<CH_3<Br and CH_3<Cl<Br, respectively) could be estimated. In other words, the size of a methyl group in comparison with those of chlorine and bromine cannot be a 'universal parameter', since the order depends on the system studied.[1f,22]

GENERAL SYNTHESES

The triol 1,3,5-tris(1-hydroxy-2,2-dimethylpropyl)-benzene (**15**), prepared according to Martinson,[3] was the starting material for the syntheses of compounds **2**, **3**, **4**, **6** and **7**. Reaction between **15** and appropriate reagents, such as thionyl chloride, thionyl bromide (in HMPT), hydrogen iodine, acetic anhydride in pyridine and trimethylsilyl chloride in pyridine gave **2**, **3**, **4**, **6** and **7** (Scheme 1).

The synthesis of 1,3,5-tris(1-fluoro-2,2-dimethylpropyl)benzene (**1**) was achieved by reaction between **2** and silver fluoride in acetonitrile.

Attempts to prepare 1,3,5-tris(1-methoxy-2,2-dimethylpropyl)benzene (**5**) from **15** by reaction with dimethyl sulphate under phase transfer catalysis conditions[23] were unsuccessful. Only one hydroxyl group

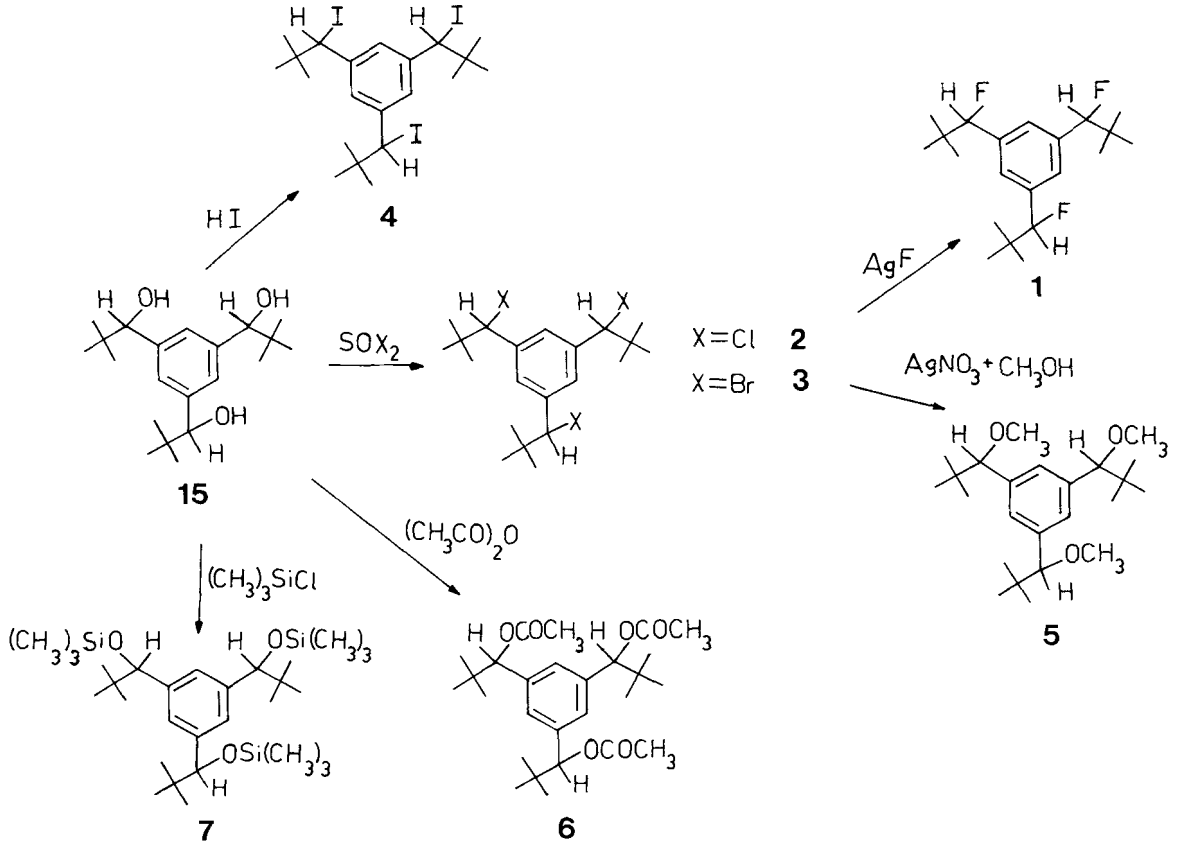

Scheme 1

was methylated (according to ^{1}H NMR) and then the reaction stopped. However if **3** was mixed with an equivalent amount of solid silver nitrate in boiling methanol, **5** was formed in nearly quantitative yield.

The precursor for the syntheses of compounds **9–14** was 1,3,5-tripivaloylbenzene (**16**), prepared according to Martinson.[3] 1,3,5-Tris(1,1-dichloro-2,2-dimethylpropyl)benzene (**10**) and 1,3,5-tris(1,1-dibromo-2,2-dimethylpropyl)benzene (**12**) were prepared by reaction between **16** and phosphorus pentachloride and phosphorus pentabromide, respectively (Scheme 2).

1,3,5-Tris(1,1-difluoro-2,2-dimethylpropyl)benzene (**9**) was prepared by reaction between **16** and the fluorinating agent diethylaminosulphur trifluoride (**17**).[24a,b,c] This fluorinating agent was prepared from sulphur tetrafluoride and diethyltrimethylsilylamine (**18**) which, in turn, was prepared from diethylamine and trimethylsilyl chloride.[24c,25]

1,3,5-Tripivaloylbenzene triethylenethioketal (**14**) was prepared from **16** and 1,2-ethanedithiol as described by Martinson.[3]

By treating **16** with methylmagnesium iodide,[3] the triol 1,3,5-tris(1-hydroxy-1,2,2-trimethylpropyl)benzene (**19**) was prepared. Reaction between this triol and thionyl chloride or hydrogen bromide gave 1,3,5-tris(1-chloro-1,2,2-trimethylpropyl)benzene (**11**) and 1,3,5-tris(1-bromo-1,2,2-trimethylpropyl)benzene (**13**), respectively.

Dehydration of **19** with phosphorus oxychloride gave the triolefin 1,3,5-tris(3,3-dimethyl-2-butenyl)benzene (**20**), which was hydrogenated (Pd,

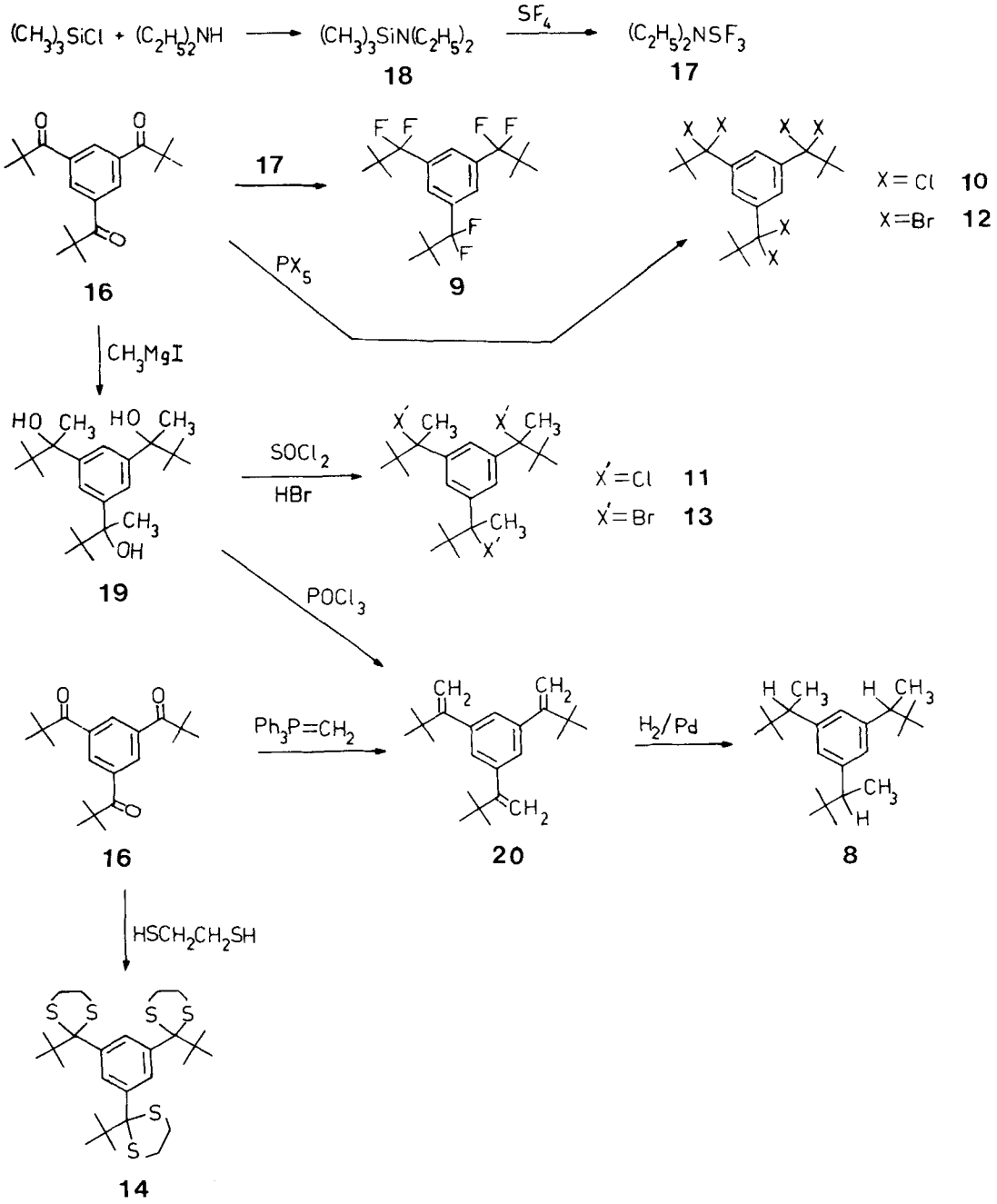

Scheme 2

10%) to 1,3,5-tris(3,3-dimethyl-2-butyl)benzene (**8**). The triolefin **20** could also be prepared by reaction between **16** and the Wittig reagent triphenylmethylene phosphorane.[26]

Preparative

^{1}H NMR spectra for identification were run on a JEOL JNM 60 spectrometer. The chemical shifts are reported in ppm downfield from tetramethylsilane. The multiplicities of the peaks are designated as singlet (s), doublet (d), triplet (t), quartet (q) and multiplet (m).

The IR spectra were run on a Perkin Elmer 257 grating infrared spectrometer using sodium chloride cells.

The mass spectra were determined on an LKB MS 9000 mass spectrometer operating with 70 eV electron energy and situated at the University of Lund. The high-resolution mass spectra were obtained on a Varian-MAT 311 mass spectrometer at the Department of Clinical Chemistry, University Hospital, Lund.

Melting points were obtained on a Kofler hot stage and are uncorrected.

Elemental analyses were performed by Analystjänst at the University of Lund.

The gas–liquid chromatographic (GLC) analyses were carried out on a Varian Aerograph 1400 gas chromatograph with a 2 m × $\frac{1}{8}$ in column packed with 3% SE-30 silicone gum rubber on Chromosorb G as the stationary phase and a flow-rate of nitrogen of 25 ml min^{-1}.

All chemicals were of reagent grade and were used without further purification, unless otherwise stated.

1,3,5-Tris(1-hydroxy-2,2-dimethylpropyl)benzene (15). M.p. 214–215 °C (lit.[3] 215 °C).

1,3,5,-Tripivaloylbenzene (16). M.p. 79–80 °C (lit.[3] 79.5–80.5 °C).

1,3,5,-Tris(1-chloro-2,2-dimethylpropyl)benzene (2). Thionyl chloride (6.4 g, 53.7 mmol) was added to **15** (2.0 g, 6.0 mmol) with cooling. The reaction mixture was then heated to 60 °C with stirring. Small samples were taken, hydrolysed and analysed by TLC (on alumina with cyclohexane as eluent). After 12 h the reaction was found to be complete, and the reaction mixture was hydrolysed with 20 ml of water and extracted with three 15 ml portions of diethyl ether. The organic phases were collected, dried ($MgSO_4$) and the solvent evaporated, leaving a brown residue, which was chromatographed on a column of alumina with cyclohexane as eluent. Collection and evaporation of the solvent left 2.2 g of a white crystalline residue, yield 99%, m.p. 158–159 °C. (Found: C 64.7; H 8.53; Cl 26.8%. Calc. for $C_{21}H_{33}Cl_3$: C 64.37; H 8.43; Cl 27.20%). ^{1}H NMR ($CDCl_3$): δ 1.03 [27H, s, $C(CH_3)_3$], 4.72 (3H, s, CHCl), 7.26 (3H, m, arom. H). IR (ν_{max}, CCl_4): 1480 cm^{-1} (C=C str.). MS [*m*/*z* (%)]: 390 (2, $M[^{35}Cl]$), 355 (3, $[M-{}^{35}Cl]$), 333 (3, [*M* − *tert*-Bu]) isotopic pattern in agreement with 3 chlorines.

1,3,5-Tris(1-fluoro-2,2-dimethylpropyl)benzene (1). **2** (3.0 g, 7.6 mmol) was dissolved in 40 ml of dry acetonitrile, silver fluoride (5.8 g, 46.0 mmol) was added and the mixture was refluxed for 36 h. After this time a ^{1}H NMR spectrum showed complete reaction. The reaction mixture was filtered, the acetonitrile evaporated, 20 ml of water added and the aqueous phase extracted with three 15 ml portions of diethyl ether. The ether was evaporated and a yellow residue was left, which was chromatographed on a column of silica with cyclohexane–methylene chloride (2 : 1) as eluent. Collection and evaporation of the solvent left 2.2 g of a white product which crystallized after a few days, yield 86%, m.p. 85–86 °C. (Found: C 73.7; H 9.42; F 16.8%. Calc. for $C_{21}H_{33}F_3$: C 73.71; H 9.65; F 16.69%). ^{1}H NMR ($CDCl_3$): δ 0.96 [27H, s, $C(CH_3)_3$], 5.14 [3H, d, CHF, *J*(HF) = 46 Hz], 7.10–7.25 (3H, m, arom. H). IR (ν_{max}, CCl_4): 1465 cm^{-1} (C=C str.). MS [*m*/*z* (%)]: 342 (3, *M*), 285 (7, [*M*-*tert*-Bu]).

1,3,5-Tris(1-bromo-2,2-dimethylpropyl)benzene (3). **15** (3.2 g, 9.5 mmol) was dissolved in 25 ml of dry HMPT, thionyl bromide (23.5 g, 113.0 mmol) was added and the mixture was stirred at room temperature. Small samples were taken and analysed by ^{1}H NMR. After 5 days the reaction was found to be complete. The reaction mixture was poured into 65 ml of water and the aqueous phase was extracted with eight 25 ml portions of hexane. The organic extractions were combined, dried ($MgSO_4$) and the solvent evaporated, leaving a brown residue which was chromatographed on a column of alumina with cyclohexane as eluent. Collection and evaporation left 2.6 g of a white crystalline residue, yield 51%, m.p. 164–165 °C (lit.[1i] m.p. 164–165 °C). ^{1}H NMR, IR and MS spectra are in accordance with those published.

1,3,5-Tris(1-iodo-2,2-dimethylpropyl)benzene (4). Dry hydrogen iodide (8.6 g, 67.2 mmol), made from reaction between 66% (sp. gr = 1.94 g l^{-1}) hydroiodic acid and an excess of phosphorus pentoxide plus a catalytic amount of red phosphorus (0.1 g), was condensed into a three-necked flask containing **15** (2.5 g, 7.4 mmol) at −60 °C. The reaction mixture was stirred at this temperature for 10 h, after which time TLC (on alumina with cyclohexane as eluent) showed complete reaction. The reaction mixture was allowed to reach room temperature, 15 ml of water was added to the semi-solid residue and the aqueous phase was extracted three times with 20 ml of benzene. Collection of the organic extracts, drying ($MgSO_4$) and evaporation of the solvent left a red solid residue which was chromatographed on a column of alumina with hexane as eluent. Collection and evaporation of the solvent left 3.3 g of a white crystalline residue, yield 67%, m.p. 168–169 °C. (Found: C 38.3; H 5.06; I 56.7%. Calc. for $C_{21}H_{33}I_3$: C 37.84; H 4.95; I 57.21%). ^{1}H NMR ($CDCl_3$): δ 1.06 [27H, s, $C(CH_3)_3$], 4.97 (3H, s, CHI), 7.14–7.20 (3H, m, arom. H). IR (ν_{max}, CCl_4): 1485 cm^{-1} (C=C str.). MS [*m*/*z* (%)]: 609 (2, [*M*-*tert*-Bu]), 539 (100, [*M* − I]).

1,3,5-Tris(1-methoxy-2,2-dimethylpropyl)benzene (5). 3 (0.83 g, 1.6 mmol) was mixed with solid silver nitrate (2.0 g, 11.9 mmol) and 40 ml of dry methanol. The reaction mixture was refluxed for 12 h until TLC (on alumina, methylene chloride as eluent) showed the reaction to be complete. The mixture was filtered, the methanol evaporated and the semi-solid yellow residue chromatographed on a column of alumina. The column was first eluted with hexane to eliminate some impurities, then with methylene chloride to elute the product. After collection and evaporation of the solvent there remained 0.5 g of a white crystalline residue, yield 76%, m.p. 72–73 °C. (Found: C 76.2; H 10.9%. Calc. for $C_{24}H_{42}O_3$: C 76.12; H 11.19%). ^{1}H NMR ($CDCl_3$): δ 0.91 [27H, s, $C(CH_3)_3$], 3.15 (9H, s, OCH_3), 3.85 (3H, s, CH), 6.86–7.11 (3H, arom. H). IR (ν_{max} CCl_4): 1100 cm^{-1} (C–O–C str.). MS [*m/z* (%)]: 378 (1, *M*), 363 (6, [*M* − CH_3]), 321 (100, [*M* − *tert*-Bu]).

1,3,5-Tris(1-acetoxy-2,2-dimethylpropyl)benzene (6). 15 (1.0 g, 3.0 mmol) was dissolved in 15 ml of dry pyridine and acetic anhydride (9.0 g, 15 mmol) was added. The reaction mixture was stirred at room temperature, and the reaction was followed by ^{1}H NMR. After 4 days NMR showed the reaction to be complete, and 30 ml of water was added to the reaction mixture. The aqueous phase was extracted twice with 10 ml of ethyl acetate. The organic phases were collected and washed three times with 10 ml of a 10% solution of sodium hydrogen carbonate, 10 ml of water, dried ($MgSO_4$) and the ethyl acetate evaporated leaving a solid residue, which was chromatographed on a column of alumina with ethyl acetate as eluent. Collection and evaporation of the ethyl acetate left 1.1 g of a white crystalline residue, yield 81%, m.p. 118–119 °C. (Found: C 70.3; H 9.21%. Calc. for $C_{27}H_{42}O_6$: C 70.13; H 9.09%). ^{1}H NMR ($CDCl_3$): δ 0.92 [27H, s, $C(CH_3)_3$,] 2.09 (9H, s, $COCH_3$), 5.54 (3H, s, CH), 7.16 (3H, s, arom. H). IR (ν_{max}, CCl_4): 1730 cm^{-1} (C=O str.). MS [*m/z* (%)]: 462 (1, *M*), 405 (2, [*M* − *tert*-Bu]), 346 (13, [*M* − *tert*-Bu − OAc]).

1,3,5-Tris(1-trimethylsilyloxy-2,2-dimethylpropyl)benzene (7). 15 (0.5 g, 1.5 mmol) was dissolved in 10 ml of dry pyridine, trimethylchlorosilane (0.98 g, 9.0 mmol) was added and the mixture was refluxed. After 24 h of refluxing ^{1}H NMR showed the reaction to be complete, and 50 ml of water was added. The aqueous phase was extracted twice with 15 ml of diethyl ether and the organic phases were collected. After washing three times with 15 ml of water, the organic phase was dried ($MgSO_4$) and the solvent evaporated. The residue was chromatographed on a column of alumina with cyclohexane as eluent. Collection and evaporation of the solvent left 0.75 g of a white crystalline product, yield 91%, m.p. 138–139 °C. (Found: C 65.7; H 11.0; Si 14.8%. Calc. for $C_{30}H_{60}O_3Si_3$: C 65.18; H 10.86; Si 15.26%). ^{1}H NMR ($CDCl_3$): δ 0 [27H, s, $Si(CH_3)_3$], 0.94 [27H, s, $C(CH_3)_3$], 4.34 (3H, s, CH), 7.10–7.21 (3H, s, arom. H). IR (ν_{max}, KBr): 1245 cm^{-1} (Si–C def.). MS [*m/z* (%)]: 552 (1, *M*), 537 (4, [*M* − CH_3]), 495 (100, [*M* − *tert*-Bu]).

Diethyltrimethylsilylamine (18). B.p. 126–127 °C/760 torr; n_D^{23} = 1.4104 (lit.[25] b.p. 126.8–127.1 °C/738 torr, 126.1–126.4 °C/760 torr; n_D^{20} = 1.4112).

Diethylaminosulphur trifluoride (17). B.p. 43–44 °C/12 torr (lit.[24a–c] b.p. 43–44 °C/12 torr).

1,3,5-Tris(1,1-difluoro-2,2-dimethylpropyl)benzene (9). 16 (2.0 g, 6.1 mmol) dissolved in 15 ml of dry carbon tetrachloride was added slowly to **17** (3.4 g, 21.1 mmol) in a three-necked flask with external cooling. The reaction mixture was then heated to reflux. After refluxing for 40 min, the reaction mixture was cooled and poured into 30 g of ice–water. The organic layer was separated and the aqueous phase extracted with three 15 ml portions of carbon tetrachloride. The organic phases were collected and the solvent evaporated, leaving a tan-coloured crystalline residue. The residue was chromatographed on a column of silica (deactivated with 10% of water) with cyclohexane as eluent. Collection and evaporation of the solvent left 2.3 g of a white crystalline product, yield 98%, m.p. 112–113 °C. High-resolution mass spectrometry gave MW = 396.2252; the value for $C_{21}H_{30}F_6$ is 396.2252. ^{1}H NMR ($CDCl_3$): δ 1.04 [27H, s, $C(CH_3)_3$], 7.49 (3H, s, arom. H). IR (ν_{max}, CCl_4) 1080 cm^{-1} (C–F str.). MS [*m/z* (%)]: 396 (5, *M*), 381 (23, [*M* − CH_3]), 339 (31, [*M* − *tert*-Bu]).

1,3,5-Tris(1,1-dichloro-2,2-dimethylpropyl)benzene (10). 16 (2.0 g, 6.1 mmol) was mixed with phosphorus pentachloride (4.8 g, 23.0 mmol) and heated to 115 °C with stirring. Small samples were taken, hydrolysed and analysed by TLC (on silica gel with cyclohexane as developer). After a reaction time of 10 h at 115 °C, the reaction was found to be complete (TLC), and the mixture was cooled, hydrolysed with 25 ml of water and extracted with four 15 ml portions of benzene. The organic phases were collected and the solvent was evaporated, leaving a brown residue. The residue was chromatographed on a column of silica (deactivated with 10% of water) with cyclohexane as eluent. Collection and evaporation of the solvent left 2.4 g of a white crystalline product, yield 82%, m.p. 196–197 °C. (Found: C 50.7; H 6.00; Cl 42.9%. Calc. for $C_{21}H_{30}Cl_6$: C 50.91; H 6.06; Cl 43.03%). ^{1}H NMR ($CDCl_3$): δ 1.20 [27H, s, $C(CH_3)_3$], 8.16 (3H, s, arom. H). IR (ν_{max}, CCl_4): 1475 cm^{-1} (C=C str.). MS [*m/z* (%)]: 493 (1, $M[5^{35}Cl + {}^{37}Cl]$), 459 (5, $M[4^{35}Cl + 2^{37}Cl] - {}^{37}Cl$). The isotopic pattern is in agreement with 6 chlorines.

1,3,5-Tris(1,1-dibromo-2,2-dimethylpropyl)benzene (12). 16 (2.0 g, 6.1 mmol) was mixed with phosphorus pentabromide (8.9 g, 20.7 mmol) and the mixture was heated to 80 °C and stirred. Small samples were taken from time to time, hydrolysed and analysed by TLC (on silica gel with methylene chloride as developer). After 5 days the reaction was found to be complete (TLC showed only one spot) and the mixture was cooled, hydrolysed with 35 ml of water and extracted with six 20 ml portions of hot benzene. The organic layers were combined and the solvent was evaporated.

A greyish crystalline residue was left, which was recrystallized from large volumes of hot ethyl acetate. After three recrystallizations there remained 1.9 g of a white crystalline product, yield 40%, m.p. 262–263 °C. (Found: C 32.5; H 4.00; Br 62.5%. Calc. for $C_{21}H_{30}H_{30}Br_6$: C 33.07; H 4.04; Br 62.99%). ^{1}H NMR ($CDCl_3$): δ 1.28 [27H, s, $C(CH_3)_3$], 8.40 (3H, s, arom. H). IR (ν_{max}, CCl_4): 1490 cm^{-1} (C=C str.). MS [*m/z* (%)]: 747 (1, $M[^{79}Br+^{81}Br]-CH_3$), 705 (1, $M[^{79}Br+^{81}Br]-$*tert*-Bu). The isotopic pattern is in accord with 6 bromines.

1,3,5-Tripivaloylbenzene trisethylenethioketal (14). M.p. 266–267 °C (lit.[3] 266–267 °C).

1,3,5-Tris(1-hydroxy-1,2,2-trimethylpropyl)benzene (19). M.p. 139–140 °C (lit.[3] 139–140 °C).

1,3,5-Tris(1-chloro-1,2,2-trimethylpropyl)benzene (11). Thionyl chloride (4.2 g, 35.5 mmol) was added with cooling to **19** (1.5 g, 4.0 mmol) in a three-necked flask. The reaction mixture was stirred and heated to 60 °C. Small samples were taken, hydrolysed and analysed by TCL (on silica gel with cyclohexane as developer). After 24 h the reaction was found to be complete and the reaction mixture was cooled, hydrolysed with 20 ml of water and extracted with three 10 ml portions of diethyl ether. Collection of the organic phases, drying (Na_2SO_4) and evaporation of the solvent left a brown residue, which was chromatographed on a column of silica (deactivated with 15% of water) with cyclohexane as eluent. Collection and evaporation of the solvent left 1.6 g of a white crystalline residue, yield 93%, m.p. 187–188 °C. (Found: C 66.8; H 9.21; Cl 24.2%. Calc. for $C_{24}H_{39}Cl_3$ C 66.44; H 9.00; Cl 24.56%). ^{1}H NMR ($CDCl_3$): δ 1.03 [27H, s, $C(CH_3)_3$], 2.10 (9H, s, CH_3), 7.67 (3H, m, arom. H). IR (ν_{max}, CCl_4): 1605 cm^{-1} (C=C str.). MS [*m/z* (%)]: 419 (4, $M[^{35}Cl+^{37}Cl]-CH_3$), 417 (4, $M[^{35}Cl]-CH_3$), 375 (18, $M[^{35}Cl]-$*tert*-Bu). The isotopic pattern corresponds to 3 chlorines.

1,3,5-Tris(1-bromo-1,2,2-trimethylpropyl)benzene (13). Dry hydrogen bromide (0.35 g, 4.3 mmol) was absorbed in a solution of **19** (0.27 g, 0.7 mmol) dissolved in 15 ml of dry benzene and the reaction mixture was stirred at room temperature. The reaction was followed by ^{1}H NMR, and after 9 h the reaction was found to be complete. Stirring was maintained for an additional 4 h and then the solvent was evaporated, leaving a brown crystalline residue which was recrystallized from hot diisopropyl ether. After three recrystallizations there remained 0.24 g of a white crystalline product, yield 60%, m.p. 188–189 °C. (Found: C 51.0; H 7.00; Br 41.9%. Calc. for $C_{24}H_{39}Br_3$: C 50.79; H 6.88; Br 42.32%). ^{1}H NMR ($CDCl_3$): δ 1.08 [27H, s, $C(CH_3)_3$], 2.29 (9H, s, CH_3), 7.63–7.85 (3H, m, arom. H). IR (ν_{max}, CCl_4): 1485 cm^{-1} (C=C str.). MS [*m/z* (%)]: 551 (2, $M[^{79}Br+^{81}Br]-CH_3$), 509 (3, $M[^{79}Br+^{81}Br]-$*tert*-Bu). The isotopic pattern corresponds to 3 bromines.

1,3,5-Tris(3,3-dimethyl-2-butenyl)benzene (20). Phosphorus oxychloride (0.73 g, 4.8 mmol) was added to **19** (0.5 g, 1.3 mmol) dissolved in 6 ml of dry pyridine, with external cooling. The reaction mixture was then refluxed for 24 h until ^{1}H NMR showed complete reaction. Then 30 ml of water were added and the aqueous phase was extracted with two 15 ml portions of cyclohexane. Collection of the organic phases, drying ($MgSO_4$) and evaporation of the solvent left a yellow viscous product, which was chromatographed on a column of alumina with cyclohexane as eluent. Collection and evaporation of the solvent left 0.41 g of an oily colourless product, yield 96%. (Found: C 88.4; H 10.9%. Calc. for $C_{24}H_{36}$: C 88.89; H 11.11%). ^{1}H NMR ($CDCl_3$): δ 1.13 [27H, s, $C(CH_3)_3$], 4.79 [3H, d, CH, *J*(HH)*gem* = 2.5 Hz], 5.16 [3H, d, CH, *J*(HH)*gem* = 2.5 Hz], 6.79 (3H, s, arom. H). IR (ν_{max} CCl_4): 3090 cm^{-1} (C–H str.). MS [*m/z* (%)]: 324 (47, *M*), 309 (57, $[M-CH_3]$).

20 could also be synthesized by adding a solution of **16** (1.0 g, 3.0 mmol) in 10 ml of dry diethyl ether to a solution of triphenylmethylene phosphine (9.1 mmol), prepared according to Ref. 26, in dry diethyl ether. Dimethyl sulphoxide (10 ml) was then added and the mixture was refluxed for 24 h. After hydrolysis with 25 ml of water, the aqueous phase was extracted with several 10 ml portions of cyclohexane. Work up and decolourization as described above gave an identical product (0.92 g), yield 93%.

1,3,5-Tris(3,3-dimethyl-2-butyl)benzene (8). 20 (1.0 g, 3.1 mmol) was dissolved in 50 ml of absolute ethanol, 10% Pd on charcoal (0.15 g) was added and the mixture was hydrogenated in a Parr apparatus at a hydrogen pressure of 490 kPa. When the theoretical amount of hydrogen had been absorbed, the reaction mixture was filtered by the use of Celite, the solvent evaporated and the residue chromatographed on a column of alumina with hexane as eluent. Collection and evaporation of the solvent left 1.0 g of a white crystalline product, yield 98%, m.p. 84–85 °C. (Found: C 87.3; H 12.7%. Calc. for $C_{24}H_{39}$; C 87.27; H 12.73%). ^{1}H NMR ($CDCl_3$): δ 0.85 [27H, s, $C(CH_3)_3$], 1.25 (9H, d, CH_3, *J* = 7 Hz), 2.53 (3H, q, CH, *J* = 7 Hz), 6.80 (3H, s, arom. H). IR (ν_{max} CCl_4) 1600 cm^{-1} (C=C str.). MS [*m/z* (%)]: 330 (9, *M*), 315 (7, $[M-CH_3]$), 273 (100, $[M-$*tert*-Bu]).

Acknowledgements

We express out thanks to Dr Robert E. Carter for stimulating discussions, comments on the manuscript and linguistic criticism. We are also grateful to Professor Börje Wickberg for his synthetic support, Dr Tommy Liljefors for placing his version of the Allinger MM1/MMP1 program at out disposal and Ms Evabritt Sandmark for typing the manuscript.

REFERENCES

1. (a) R. E. Carter, J. Marton and K. I. Dahlqvist, *Acta Chem. Scand.* **24**, 195 (1970); (b) B. Nilsson, R. E. Carter, K. I. Dahlqvist and J. Marton, *Org. Magn. Reson.* **4**, 95 (1972); (c) B. Nilsson, *Mol. Phys.* **27**, 625 (1974); (d) B. Nilsson, P.

Martinson, K. Olsson and R. E. Carter, *J. Am. Chem. Soc.* **95,** 5615 (1973); (e) B. Nilsson and T. Drakenberg, *Org. Magn. Reson.* **6,** 155 (1974); (f) B. Nilsson, P. Martinson, K. Olsson and R. E. Carter, *J. Am. Chem. Soc.* **96,** 3190 (1974); (g) R. E. Carter, B. Nilsson and K. Olsson, *J. Am. Chem. Soc.* **97,** 6155 (1975); (h) E. Dahlberg, B. Nilsson, K. Olsson and P. Martinson, *Acta Chem. Scand. B* **29,** 300 (1975); (i) S. Andersson, R. E. Carter and T. Drakenberg, *Acta Chem. Scand. B* **34,** 661 (1980); (j) R. E. Carter and P. Stilbs, *J. Am. Chem. Soc.* **98,** 7515 (1976).

2. J. M. A. Baas and A. Sinnema, *Recl. Trav. Chim. Pays-Bas* **92,** 899 (1973).
3. P. Martinson, *Acta Chem. Scand.* **23,** 751 (1969).
4. (a) J. Peeling, J. B. Rowbotham, L. Ernst and T. Schaefer, *Can. J. Chem.* **52,** 2414 (1974); (b) U. Berg and U. Sjöstrand, *Org. Magn. Reson.* **11,** 555 (1978).
5. S. Glasstone, K. J. Laidler and H. Eyring, *The Theory of Rate Processes,* p. 195. McGraw-Hill, New York (1941).
6. G. Binsch, in *Dynamic Nuclear Magnetic Resonance Spectroscopy,* edited by L. M. Jackman and F. A. Cotton, pp. 45–76. Interscience, New York (1975).
7. (a) N. L. Allinger, M. T. Tribble, M. A. Miller and D. H. Wertz, *J. Am. Chem. Soc.* **93,** 1637 (1971); (b) D. H. Wertz and N. L. Allinger, *Tetrahedron* **30,** 1597 (1974); (c) N. L. Allinger, J. T. Sprague and T. Liljefors, *J. Am. Chem. Soc.* **98,** 5100 (1974); (d) N. L. Allinger and J. T. Sprague, *J. Am. Chem. Soc.* **95,** 3893 (1973); (e) T. Liljefors and N. L. Allinger, *J. Am. Chem. Soc.* **98,** 2745 (1976); (f) R. E. Carter and T. Liljefors, *Tetrahedron* **32,** 2915 (1976); (g) A. Meyer and N. L. Allinger, *Tetrahedron* **31,** 1971 (1975).
8. MM1/MMP1 program (QCPE, No. 318).
9. J. D. Roberts and M. Caserio, *Basic Principles of Organic Chemistry,* p. 592. Benjamin, New York (1965).
10. S. Andersson and T. Drakenberg, *Org. Magn. Reson.* in press.
11. For examples see *Bruker ^{13}C Data Bank, Vol. 1.* Bruker Physik, Maisch OHG, Karlsruhe, Germany (1976).
12. J. E. Anderson, H. Pearson and D. I. Rawson, *J. Chem. Soc., Chem. Commun.* 95 (1973).
13. A. Rieker and H. Kessler, *Tetrahedron Lett.* 1227 (1969).
14. A. Meyer, *J. Mol. Struc.* **40,** 127 (1977).
15. N. L. Allinger, *J. Am. Chem. Soc.* **99,** 8127 (1977).
16. W. Freitag and H. J. Schneider, *Isr. J. Chem.* **20,** 153 (1980).
17. B. L. Hawkins, B. Bremser, S. Borcic and J. D. Roberts, *J. Am. Chem. Soc.* **93,** 4472 (1971).
18. (a) J. E. Anderson and H. Pearson, *Tetrahedron Lett.* 2779 (1972); (b) J. E. Anderson and H. Pearson, *J. Chem. Soc., Chem. Commun.* 871 (1971); (c) J. E. Anderson and H. Pearson, *J. Am. Chem. Soc.* **97,** 764 (1975); (d) J. E. Anderson and H. Pearson, *J. Chem. Soc. B* 1209 (1971); (e) J. E. Anderson and H. Pearson, *J. Chem. Soc., Chem. Commun.* 908 (1972).
19. F. Imashiro, T. Terao and A. Saiko, *J. Am. Chem. Soc.* **101,** 3762 (1979).
20. MM2 program (QCPE, No. 395).
21. H. D. Beckhaus, C. Ruckardt and J. E. Anderson, *Tetrahedron* **38,** 2299 (1982).
22. D. Hounshell, L. Iroff, D. Iversen, R. Wroczynski and K. Mislow, *Isr. J. Chem.* **20,** 65 (1980).
23. A. Merz, *Angew. Chem.* **85,** 868 (1973).
24. (a) L. Markovskij, V. Pashinnik and A. Kirsanov, *Synthesis* 787 (1973); (b) S. P. von Halasz and O. Glemser, *Chem. Ber.* **103,** 594 (1970); (c) W. J. Middleton and E. M. Bingham, *Org. Synth.* **57,** 50.
25. S. Langer, S. Connell and I. Wender, *J. Org. Chem.* **23,** 50 (1978), and references cited therein.
26. G. Wittig, *Org. Synth.* Coll. Vol. 1, 530.

Received 10 March 1983; accepted 28 March 1983